

**TRAPPING OF VOLATILES AND TRACE ELEMENTS DURING CRYSTALLIZATION OF A MAGMA OCEAN.** S. Hier-Majumder<sup>1</sup> and M.M. Hirschmann<sup>2</sup>, Dept. of Earth Sciences, Royal Holloway University of London, Egham, Surrey, UK *sashgeophysics@gmail.com*, <sup>2</sup>Dept. Earth Science, U. Minnesota, Minneapolis, MN 55455 *mmh@umn.edu*

**Introduction:** The early distribution of volatiles is one of the primary determinants of subsequent evolution of terrestrial planets, affecting both internal dynamics (via viscosity and loci of melting) and the potential to shelter key volatile species from early catastrophic loss processes. The abundance of volatiles in atmospheres overlying a magma ocean modulates heat loss, and therefore has a first-order control on the time scale of MO crystallization and planetary thermal evolution [1,2].

Crystallization of a magma ocean, if perfectly efficient in segregating melt from crystals, could produce a volatile-poor solidified mantle, with retention only in nominally anhydrous silicates [3] or, under some circumstances, volatile-rich accessory phases (carbide, diamond, etc.) [4,5]. But inefficient crystal-melt segregation can potentially sequester significant volatiles in the solidified mantle. Further, because the efficiency of segregation depends on crystallization rate [6,7], there may be a feedback between MO crystallization rate and the partitioning of volatiles between the MO and its overlying atmosphere.

Previously, models of MO solidification have considered the role of convective motions in keeping crystals in suspension [8], but relatively little attention has been paid to expulsion of melt from deformable piles of crystals accumulating at the bottom or top of solidifying MO. Solomatov [7] argued that crystallization of a MO is sufficiently rapid (whole-mantle crystallization in 200 yrs) that crystal-melt separation is wholly ineffective. Elkins-Tanton [9] assumed that a constant fraction of 1% melt is trapped in the cumulate pile.

Studies of layered mafic intrusions have long documented that liquid separation from crystallizing cumulate mushes is inefficient and depends on crystallization rate [7,10,11], with trapped liquid fractions reaching ~40% for rapidly solidified regions. Here we examine the role of dynamic trapping of silicate liquid during magma ocean solidification on the volatile distribution during crystallization of a terrestrial magma ocean.

**Methods:** We consider a 1-D model of a crystallizing and cooling planet in which there are three volatile reservoirs, solid and liquid mantle and an overlying atmosphere. The heat flux,  $F$ , from the cooling planet is controlled by the temperature,  $T$ , and the composition-dependent thermal emissivity,  $\epsilon$ , of the atmosphere

$$F = \sigma\epsilon(T^4 - T_\infty^4), \quad (1)$$

where  $\sigma$  is the Stefan-Boltzmann constant. Partitioning of H<sub>2</sub>O and CO<sub>2</sub> between magma and atmospheres, taken from solubility laws, and between magma and crystallized silicates are taken from published experiments. As the MO solidifies, volatiles are incorporated as both trapped melt and in nominally anhydrous silicates. Following McKenzie [7], we employ a simple scaling relationship between the trapped melt fraction  $F_{tr}$ , the rate of secular cooling  $dT/dt$ , average matrix sedimentation velocity,  $w$ , and the disaggregation melt fraction,  $\phi_c$ , as

$$F_{tr} = \frac{\delta\phi_c}{w\Delta T} \frac{dT}{dt} \quad (2)$$

where  $\delta$  is the compaction length, and  $\Delta T$  is the depth dependent difference between liquidus and solidus temperatures within the freezing front. The scaling relation portrays the competition between compaction and cooling. For example, if the compaction length is small or matrix sedimentation velocity is large, less melt is trapped within the freezing front. If the secular cooling rate is high, in contrast, a large melt fraction can be trapped within the freezing front.

**Results:** Two cases are examined – models in which the fraction is allowed to vary according to Eqn. (2) and a reference case in which the trapped melt fraction is assumed to be constant at 0.01. Fig. 1 shows the evolution of coupled MO and overlying atmospheres for two extreme (volatile rich and poor) cases. Solidification times vary from ~0.1-4.5 Ma. Initially, most H<sub>2</sub>O is dissolved in the MO, and, owing to much lower magmatic solubility, the atmosphere consists chiefly of CO<sub>2</sub> which provides most of the initial greenhouse insulation. With increasing solidification, greater portions of H<sub>2</sub>O are degassed. Compared to the reference case, significantly more H<sub>2</sub>O and CO<sub>2</sub> are retained in the solidified mantle.

In Fig. 2, we compare the results of coupled magma ocean/atmosphere solidification simulations for systems with between 1 and 10 terrestrial oceans of H<sub>2</sub>O and a CO<sub>2</sub>/H<sub>2</sub>O mass ratio of unity. Times to completion of crystallization range from 1.5-4.2 Ma, depending on the total volatile contents. All dynamic

models produce crystallized mantles with 6-8 % trapped melt fraction. Thus, all models produce initially solidified mantles with non-negligible H and C. For example, beginning with 1 total ocean of  $H_2O$  (less the Earth's present inventory in the bulk silicate Earth), the solidified mantle has  $\sim 100$  ppm  $H_2O$ , similar to the present-day concentration of the MORB source. Owing to lower magmatic solubilities,  $CO_2$  concentrations are commensurately less;  $\sim 12$  ppm for the driest model depicted in Fig. 1.

**Mantle H/C ratio** A significant conundrum of the modern Earth is the comparatively C-rich, low H/C ratio of the bulk mantle which has previously been attributed either to massive subduction of C through time or to precipitation of a C-rich phase during magma ocean solidification [4,5,12]. Dynamic trapping of melt during MO solidification can resolve these melt trapping can produce a residual mantle with volatile abundances and H/C ratios similar to modern Earth's

mantle (0.5-0.75 [12]) provided initial bulk volatiles are similar to chondrites (H/C  $\sim 0.2$  [12]).

Although our models were motivated chiefly to understand major volatiles, they may also be applied to distributions of other incompatible elements following magma ocean crystallization, including rare gases, heat-producing elements, and key fractionations such as Sm/Nd.

**References:** [1] Abe, Y. (1997) *PEPI* 100 27-39. [2] Zahnle, K.J. et al. (1988) *Icarus* 74 62-97. [3] Kawamoto, T. et al. (1996) *EPSL* 142 587-592. [4] Hirschmann M.M. (2012) *EPSL* 341 48-57/ [5] Dasgupta et al. (2013) *GCA* 102 191-213. [6] Solomatov 2000 [7] McKenzie, D. (2011) *J. Pet.* 52 905-930. [8] Suckale J. et al. (2012) *JGR* 117 E08005. [9] Elkins-Tanton [10] Wager L.R. et al. (1960) *J. Pet.* 1 73-85. [11] Tegner C. et al. (2009) *J. Pet.* 50 813-840. [12] Hirschmann M.M. & Dasgupta R. (2009) *Chem. Geol.* 262 4-16..

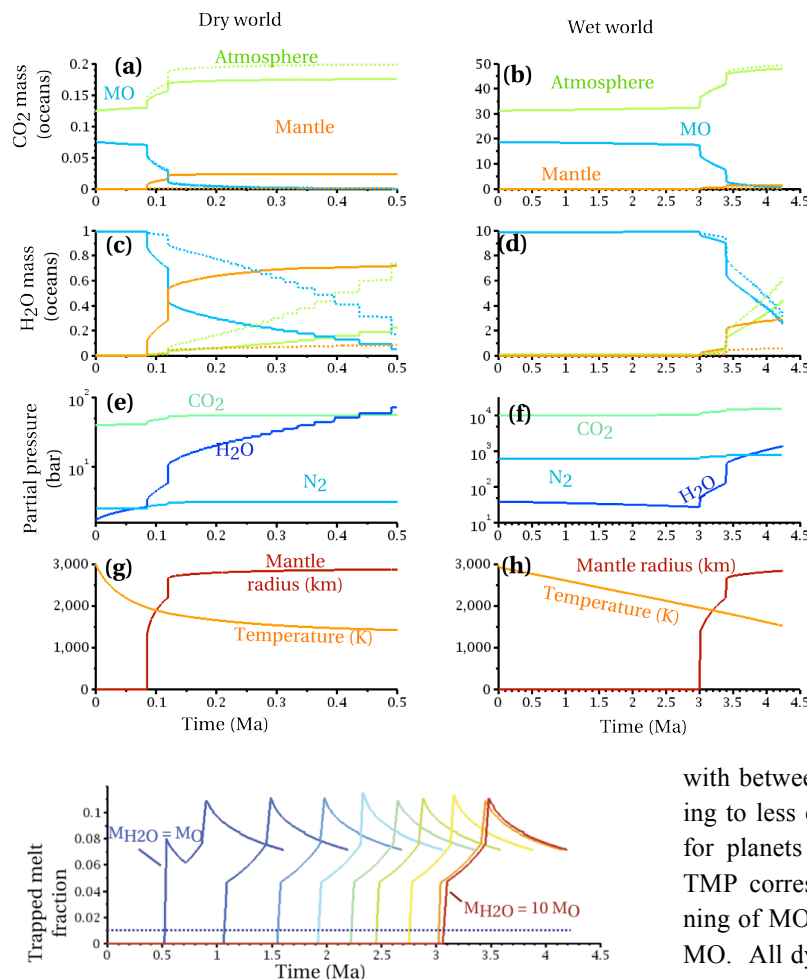


**Fig. 1** Evolution of the major volatile reservoirs in a terrestrial planet for extreme volatile-rich and volatile-poor magma ocean /atmosphere systems. (Left panels) 1, 0.2, and 0.01 ocean masses of  $H_2O$ ,  $CO_2$ , and  $N_2$ , lead to 90% crystallization of the magma ocean in 100 ka. Broken curves correspond to volatile masses calculated using a constant trapped liquid fraction.  $CO_2$  is degassed relatively early, creating a thick  $CO_2$ -rich initial atmosphere. For the volatile-poor case, the partial pressure of  $H_2O$  exceeds  $CO_2$  (panel e) by 500 ka. (Right panels) 10 oceans worth of  $H_2O$  and 50 oceans of  $CO_2$ , with 2.5 oceans of  $N_2$ , prolong 90% crystallization period to 3.5 Ma.

**Fig. 2** Average trapped melt fraction (TMP) for a solidifying MO for planets

with between 1 and 10 oceans of  $H_2O$  and  $CO_2$ . Owing to less efficient cooling, solidification begins later for planets with greater volatile budgets. Spikes in TMP correspond to rapid solidification at the beginning of MO crystallization and in crystallization of the MO. All dynamic simulations end with mean TMP of 6-8 %, substantially greater than the 1% assumed in a simple non-dynamic reference model.